# High-Speed InGaAlAs–InAlAs MQW Directional Coupler Waveguide Switch Modules Integrated with a Spotsize Converter Having a Lateral Taper, Thin-Film Core, and Ridge

Masaki Kohtoku, Kenji Kawano, Satoshi Sekine, Hiroaki Takeuchi, Naoto Yoshimoto, *Member, IEEE*, Masato Wada, *Member, IEEE*, Toshio Ito, Mitsuaki Yanagibashi, Susumu Kondo, Yoshio Noguchi, and Mitsuru Naganuma, *Member, IEEE*

***Abstract*—Fully packaged $2 \times 2$ and $4 \times 4$ semiconductor optical switch modules are successfully developed by integrating spotsize converters (SSC's) consisting of lateral tapers, thin-film cores, and ridges in InGaAlAs–InAlAs muliple quantum-well (MQW) directional coupler waveguide switches in the 1.55-$\mu$m wavelength region. Good reproducibility is obtained for the perfect coupling length of the directional coupler by appropriately designing the ridge width and gap of strip-loaded optical waveguides and by making use of the $Cl_2$ reactive-ion-beam-etching and successive wet-etching. Since the switching time is sufficiently short ($<$70 ps, which is limited by the driver speed) for the $4 \times 4$ switch module, no bits are lost during a 10-Gb/s switching experiment at a wavelength of 1.55 $\mu$m.**

***Index Terms*—Module, optical switch, quantum confined Stark effect, semiconductor switches, spotsize converter (SSC).**

## I. Introduction

FIBER optical communication is developing rapidly and its applications now range from long-distance transmission to high-speed broad-band interconnected networks. Consequently, there is an increasing need for optical switch matrices for routing, cross connection, add–drop multiplexing, and so on. High speed optical switches are especially necessary for packet switching, demultiplexing, and uninterruptive switching. The recent progress in wavelength-division-multiplexed (WDM) lightwave communication systems will further increase the necessity of optical-switch [1] modules. Several optical-switch architectures have been proposed and implemented in silica on silicon or glass substrates[2], lithium-niobate[3], and semiconductors[4]–[16]. The planar lightwave circuit (PLC) can be used to develop large-scale matrix switches with good performance [2], however, these switches are slow. Lithium-niobate switches, on the other hand, are fast, but they have large polarization dependence, and are impossible to monolithically integrate with active devices. On the other hand, InP-based matrix switches have a clear advantage because of their potential for large scale and monolithic integration with devices, such as lasers, amplifiers, detectors, and other electronic driving circuits. As for semiconductor-based switches, various types have been proposed. Semiconductor optical-amplifier gate-type switches [9], [10] exhibit low insertion loss, or even net gain, and quite high-extinction ratios. However, have the disadvantage of the switching speed, which is limited by the carrier lifetimes in the order of nanoseconds. The carrier lifetime also causes the pattern effect, which result in signal degeneration. In contrast above mentioned, switches using the quantum-confined Stark effect (QCSE) are good candidates because of their large refractive index change and high speed [17].

On the other hand, since the spotsizes of semiconductor waveguides are much smaller than those of single-mode fibers (SMF's), they need to be magnified to reduce the coupling loss between the waveguides and the plane-ended SMF's and to achieve large misalignment tolerances for the plane-ended SMF's. Since arrayed fibers are used in optical waveguide switches, compact and efficient spotsize converters (SSC's) [18]–[24] are needed.

This paper describes $2 \times 2$ and $4 \times 4$ directional-coupler waveguide-switch modules integrated with a SSC [18]–[22], which has a lateral taper, thin-film core, and wide ridge. The thin-film core confines the propagating field in the vertical direction, while the ridge confines it in the horizontal direction. Good reproducibility is obtained for the perfect coupling length of the directional coupler by appropriately designing the ridge width and gap of strip-loaded optical waveguides and by making use of the $Cl_2$ reactive-ion-beam-etching ($Cl_2$-RIBE) and successive wet-etching. Since the operating wavelength of the switches is 1.55 $\mu$m, the exciton absorption peak wavelength is determined to be 1.44 $\mu$m for the $2 \times 2$ directional coupler waveguide switch module [18]–[20]. The respective thicknesses for the InGaAlAs wells and InAlAs barriers were designed to be 9 and 5 nm. For the $4 \times 4$ directional coupler waveguide switch module [21], [22], the optical field propagates farther than it does for the $2 \times 2$ switch module. Thus, the exciton absorption peak wavelength was set at 1.40 $\mu$m to suppress the propagation loss increase caused by the exciton absorption. The 13-nm-wide well was used to decrease the driving-voltage increase caused by the shorter wavelength of

Manuscript received November 3, 1999; revised April 10, 1999.

The authors are with the NTT Photonics Laboratories, Atsugi-Shi, Kanagawa 243-0198, Japan.

Publisher Item Identifier S 0733-8724(00)02187-3.

the exciton absorption peak. Integration of the SSC's enables us to fabricate $2 \times 2$ and $4 \times 4$ optical switch modules with a UV-cure adhesive.

The connector-to-connector insertion loss, crosstalk ,and driving voltage are respectively around 15 dB, $< -20$ dB, and 7.0 V for the $2 \times 2$ switch modules and around 19 dB, $< -13$ dB, and $<10$ V for the $4 \times 4$ switch modules. Since the switching speed is sufficiently fast ($<70$ ps), no bits of a 10-Gb/s optical signal were lost for the $4 \times 4$ switch module during a switching experiment at a wavelength of 1.55 $\mu$m [22].

Section II briefly describes the structures of $2\times2$ and $4\times4$ optical waveguide switches and the design procedure. Section III explains the fabrication, and Section IV discusses the measured characteristics for the SSC's, switch chips, and switch modules.

## II. Structure and Design

Fig. 1(a) and (b), respectively, shows a bird's-eye view of a $2 \times 2$ optical waveguide switch and a top view of a $4 \times 4$ optical waveguide switch. Conventional optical directional couplers with strip-loaded optical waveguides were used, and the Benes network architecture was applied to the $4 \times 4$ switches, where six $2 \times 2$ switch elements were used. To expand the spotsizes of the semiconductor optical waveguides to those of polarization-maintaining SMF's (PANDA SMF's), whose spotsize was 4.1 $\mu$m, the SSC's with lateral tapers, thin-film cores, and ridges were integrated in the input and output ports of the switches. The lengths of the $2 \times 2$ and $4 \times 4$ optical waveguide switches are, respectively, 6 mm and 1.65 cm.

### A. Switching Section

A cross-sectional view of the switching section, i.e., the directional coupler section, is shown in Fig. 2. Since operation under transverse electric (TE)-polarized conditions is assumed, electron-to-heavy-hole exciton absorption was used. In actual fabrication, the $2\times2$ optical waveguide switches are first processed, and then the $4 \times 4$ optical waveguide switches are fabricated.

Fig. 3(a) shows the measured propagation loss increase as a function of the detuning wavelength between the operating and the exciton absorption peak wavelengths. The plots indicate the measurement points and the hatched region shows the loss variation. Fig. 3(b) shows the measured results of the product of the half-wavelength voltage and interaction length ($V\pi \bullet L$) as a function of well width, where the parameters are the detuning wavelength and the sample length of 700 $\mu$m. Note that refractive index change caused by QCSE has a nonlinear function for the applied voltage. The required phase shift for the directional coupler switch is equal to $\sqrt{3\pi}$. And the sample length is chosen as 700 $\mu$m since the interaction length for the directional coupler-type switch is 1200 $\mu$m. Therefore the half-wavelength voltage and interaction length ($V\pi \bullet L$) of 5 V $\bullet$ mm results in the driving voltage of 7.2 V. The barrier width was the same in all cases (5 nm). Since the operating wavelength of the switches is 1.55 $\mu$m, the exciton absorption peak wavelength was determined to be 1.44 $\mu$m from Fig. 3(a) and (b) for the $2\times2$ optical waveguide switch. The thicknesses for the InGaAlAs wells and InAlAs barriers were designed to be 9 and 5 nm, respectively.

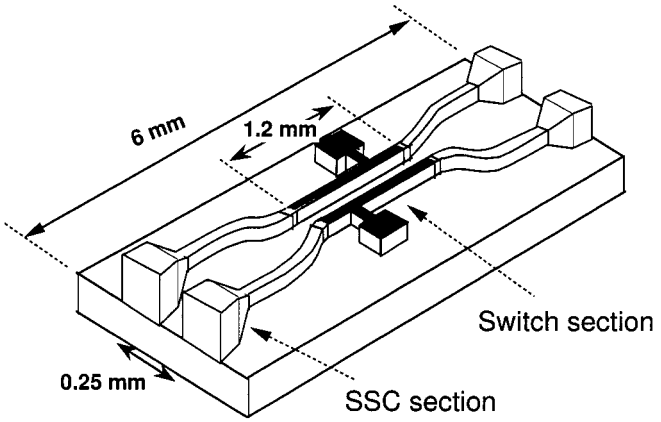


(a)

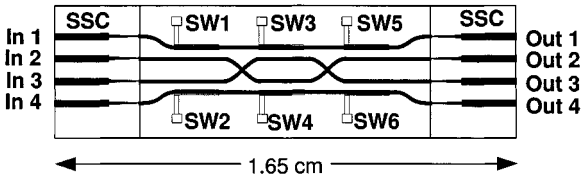


(b)

Fig. 1. (a) Bird's-eye view of a $2 \times 2$ optical waveguide switch and (b) top view of a $4 \times 4$ optical waveguide switch.

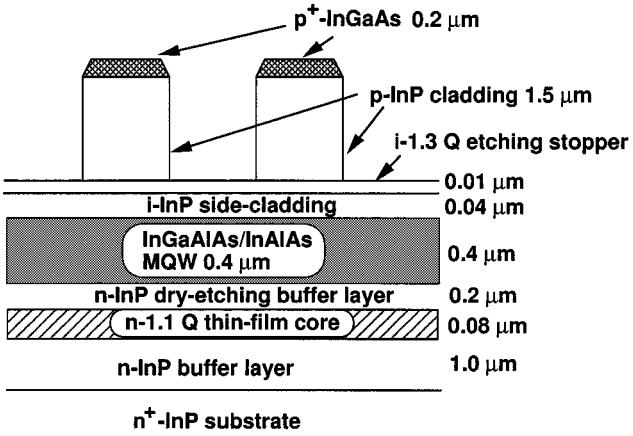


Fig. 2. Cross-sectional view of the directional coupler.

As shown in Fig. 3(a), the $2 \times 2$ optical waveguide switch suffers from a slight loss increase due to exciton absorption. The optical field propagates farther in the $4 \times 4$ switch than it does in the $2 \times 2$ optical waveguide switch. In order to suppress the effect of exciton absorption, the detuning wavelength between the operating wavelength (1.55 $\mu$m) and the exciton absorption peak wavelength has to be larger than 0.11 $\mu$m. Thus, the exciton absorption peak for the $4\times4$ switch was set at 1.40 $\mu$m to reduce propagation loss caused by the exciton absorption. However, the driving voltage will be increased as shown in Fig. 3(b). As shown in this figure, the driving voltage can be decreased by using wider wells. Hence, the InGaAlAs well width of 13 nm was chosen.

The next step is to determine the structural parameters of the optical directional coupler waveguide. The MQW primary core was determined to be 0.4 $\mu$m thick considering the confinement

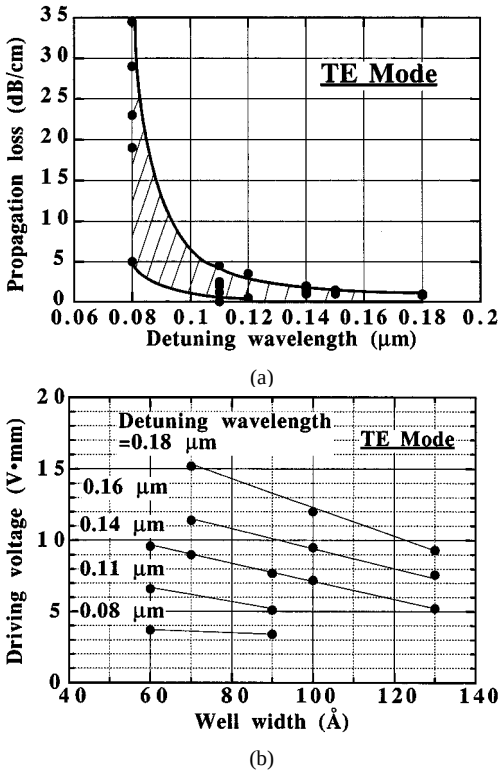


Fig. 3. (a) Propagation loss increase as a function of detuning wavelength between the operating and the exciton absorption peak wavelengths and (b) driving voltage ($Vsw$) as a function of well width, where the parameter is the detuning wavelength.

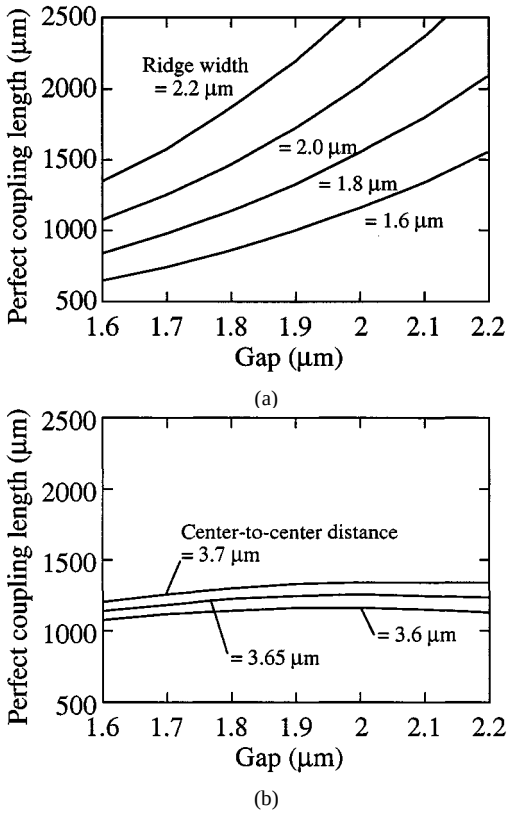


Fig. 4. (a) Calculated perfect coupling length as a function of the gap of the directional coupler, where the parameter is the ridge width of the directional coupler. (b) Calculated perfect coupling length as a function of the gap, where the parameter is the center-to-center distance of two waveguides for the directional coupler, and the ridge width is varied from 1.4 to 2.2 $\mu$m.

factor (64%) of the optical field in the MQW primary core and the perfect coupling length of 1.2 mm.

Fig. 4(a) shows the calculated perfect coupling length as a function of the gap of the directional coupler. The perfect coupling length was calculated by the finite element method [25], where the parameter is the ridge width of the strip-loaded optical waveguides. Although the perfect coupling length of the directional coupler is very sensitive to the gap for a fixed ridge width as shown in this figure, the structural parameters should be determined so that good reproducibility for the directional couplers can be obtained.

Fig. 4(b) illustrates the concept mentioned above. It shows the calculated perfect coupling length as a function of the gap of the directional coupler, where the parameter is the center-to-center distance between the two waveguides of the directional coupler and the width of the ridge is varied from 1.4 to 2.2 $\mu$m. Even if the ridge width is varied, the tolerance of the coupling length is relatively large as long as the center-to-center distance between the two optical waveguides is constant. This is because when the ridge becomes narrower, the optical field expands, which reduces the perfect coupling length. However, when the ridge narrows, the gap between two ridges widens as long as the center-to-center distance between two optical waveguides is constant. This increases the perfect coupling length. Thus, the influences caused by the variations of the ridge width and gap cancel each other out. This cancellation can also occur for the opposite case, in which the ridge is wider and gap is narrower when the center-to-center distance between two optical

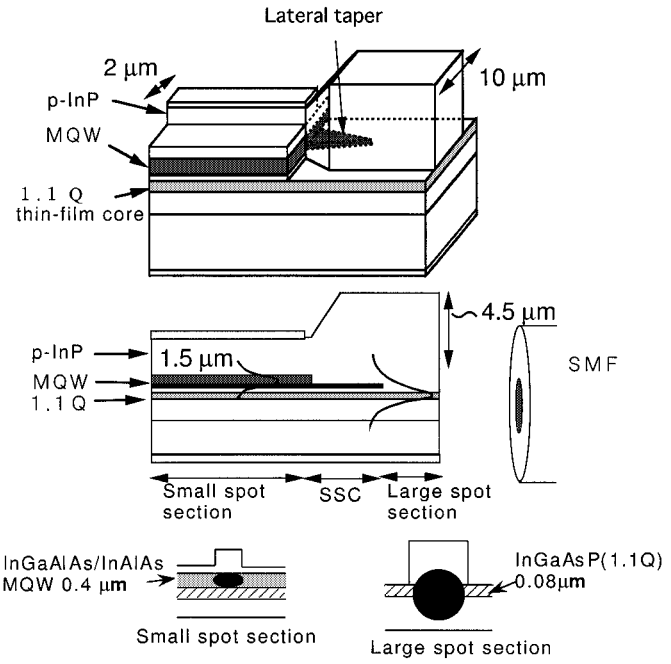


Fig. 5. Schematic views of the SSC section.

waveguides is constant. Since a stepper for 2-inch wafers was used for patterning the photoresist and $Cl_2$-RIBE and successive wet-etching were used in the fabrication, we assumed that

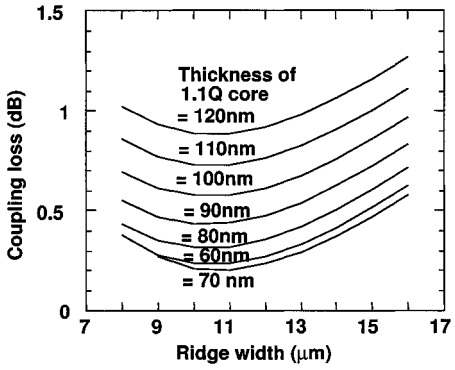


(a)

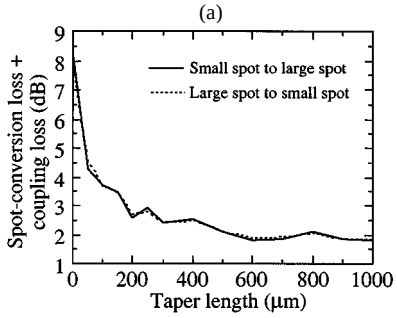


(a)

Fig. 6. (a) Calculated coupling loss as a function of the ridge width for the SSC, where the parameter is the thickness of the 1.1 Q thin-film core and (b) calculated coupling loss as a function of the taper length.

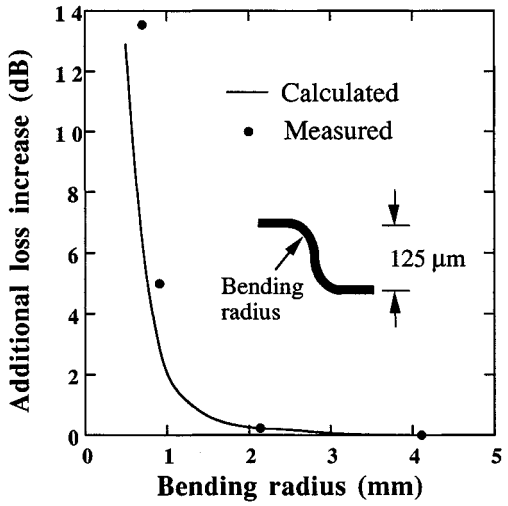


Fig. 7. Additional loss increase as a function of bending radius.

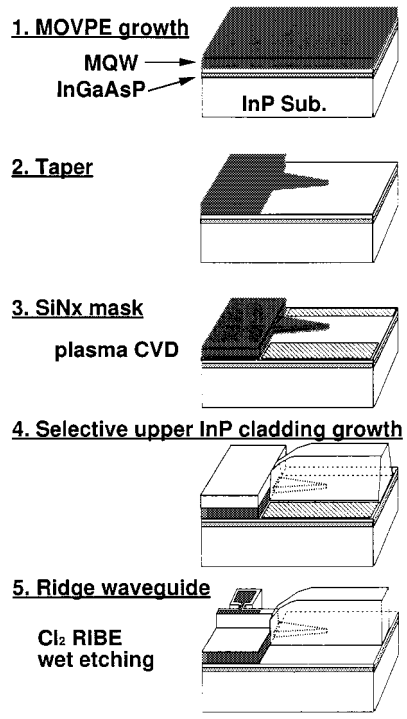


Fig. 8. Schematical diagram of the fabrication procedure of optical waveguide switches.

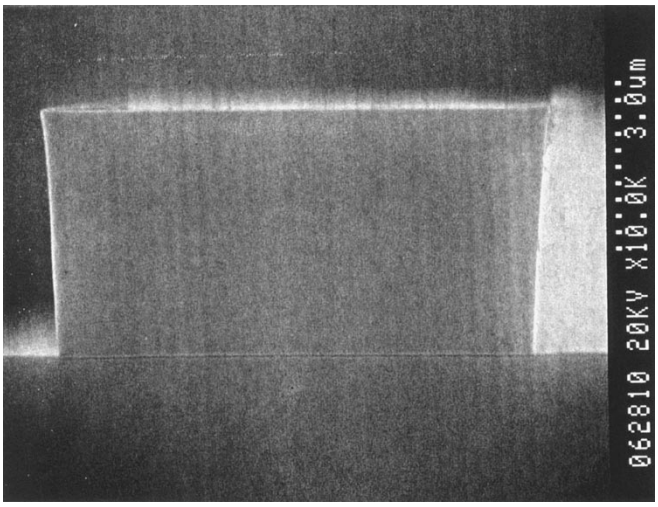


Fig. 9. SEM photograph for the endface of the SSC.

the variation of the center-to-center distance between two optical waveguides was small. Thus, good reproducibility of the directional couplers can be achieved in actual fabrication.

### *B. SSC Section*

Fig. 5 shows a schematic view of the SSC section. As shown in the figure, the MQW primary core, which is etched down from a thickness of 0.4 to 0.15 $\mu$m, is laterally tapered off in the SSC section. As the transversal crosssection of the MQW lateral taper becomes smaller in the longitudinal direction, the propagating optical beam is expanded. Next, the expanded field transfers to the 1.1 Q thin-film core. The optical field with large spotsize is confined by the thin-film core in the vertical direction and by the ridge in the horizontal direction.

The coupling loss between the SSC's and SMF's was estimated by using the finite element analysis [25]. Fig. 6(a) shows the calculated coupling loss as a function of the width of the large ridge in the SSC, where the parameter is the thickness of the 1.1 Q thin-film core. A small coupling loss of less than 0.5 dB is expected for a 1.1 Q thin-film core approximately 0.08 $\mu$m thick and a ridge approximately around 10 $\mu$m wide. Fig. 6(b) shows the calculated coupling loss as a function of the taper length. The lengths of the tapered and untapered regions were set at 300 and 200 $\mu$m, respectively.

The center-to-center distance between the SSC's, which was made to agree with the center-to-center distance between ar-

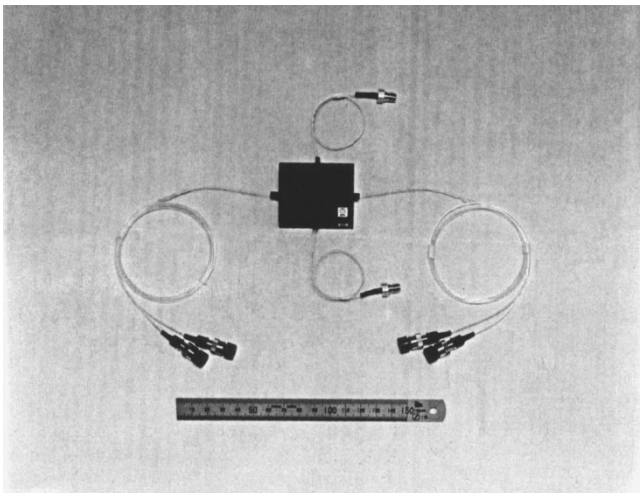

(a)

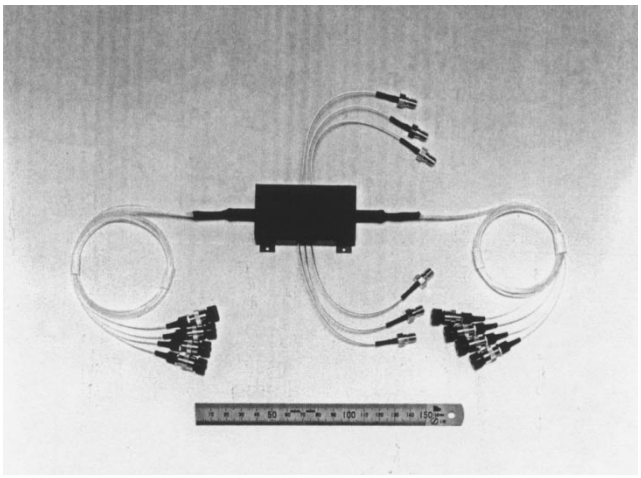

(b)

Fig. 10. (a) Photograph of the $2 \times 2$ switch module and (b) photograph of the $4 \times 4$ switch module.

rayed PANDA SMF's, was set at 250 $\mu$m for module fabrication.

### C. Waveguide Bending

As mentioned above, the center-to-center distance between the SSC's (250 $\mu$m) is much wider than that in the directional coupler region in the actual optical waveguide switches. Thus, waveguide bending is indispensable. Fig. 7 shows the additional loss increase as a function of the bending radius, where the solid line is the calculation based on the BPM and symbols are the measured results. Since the center-to-center distance between the SSC's is 250 $\mu$m, the waveguide offset was assumed to be 125 $\mu$m. As shown in this figure, a bending radius longer than 2 mm does not bring about an additional loss increase. Waveguide bending with a 4-mm radius is used for the present switch.

## III. Fabrication

The procedure for fabricating optical waveguide switches is shown in Fig. 8 is explained as follows.

1) The epitaxial layers are grown by metal organic vapor phase epitaxy on an n-doped InP substrate. The layers are a 1-$\mu$m-thick n-InP cladding layer, 0.08-$\mu$m-thick n-1.1 Q thin-film secondary core layer, and 0.2-$\mu$m-thick n-InP buffer layer for $Cl_2$-RIBE, whose doping levels are $5 \times 10^{17}$ cm$^{-3}$. Next, a 0.4-$\mu$m-thick i-InGaAlAs–InAlAs MQW primary core layer ($<10^{16}$ cm$^{-3}$) is grown.
2) After the MQW primary core layer is etched down from a thickness of 0.4 to 0.15 $\mu$m by wet-etching, the tapered section is formed to a length of 300 $\mu$m by $Cl_2$-RIBE. A SiNx film is then deposited and patterned in the SSC section for selective growth. The width and window of SiNx film patterns are 90 and 30 $\mu$m, respectively.
3) A 0.04-$\mu$m-thick i-InP side-cladding layer, 0.01-$\mu$m-thick i-1.3 Q etch-stop layer, 1.5-$\mu$m-thick p-InP cladding layer ($2 \times 10^{17}$ to $5 \times 10^{17}$ cm$^{-3}$), and 0.2-$\mu$m-thick p-cap layer ($2 \times 10^{18}$ cm$^{-3}$) are grown. At this step, a p-InP cladding layer approximately 4.5-$\mu$m thick is also grown automatically in the SSC section by selective growth with a SiNx mask.
4) After the p-electrode is deposited, strip-loaded optical waveguides are formed by $Cl_2$-RIBE and successive wet-etching. Next, the grooves are formed for electrical isolation.
5) The wafers are then cleaved into samples approximately 1 cm$^2$. After these samples are thinned and the n-electrode is formed, they are cleaved to make suitable facets for fiber coupling. AR coatings are then deposited on both endfaces of the SSC waveguides to reduce Fresnel reflections.
6) Finally, a coplanar waveguide (CPW) electrode for microwave feeding and Au-wire bonding are set up and plane-ended-arrayed-PANDA SMF's with spotsizes of 4.1-$\mu$m (in radius) are butt-coupled by using UV-cure adhesive. Since the spotsizes of the switches are expanded and coupling tolerance is enhanced by integrating the SSC's in the input and output ports, switch modules can be easily assembled with good reproducibility.

Fig. 9 shows a SEM photograph of the endface of the SSC, where the 1.1 Q thin-film core can be observed. Fig. 10(a) and (b) is a set of photographs of the $2 \times 2$ and $4 \times 4$ switch modules.

## IV. Measured Characteristics

The devices were measured by focusing an 1.55 $\mu$m light from a DFB-LD. And a polarization maintained fiber (PANDA) was used to assure the input of the TE polarized light.

### A. Spotsize Conversion by SSC

Fig. 11 compares the measured near-field patterns for a field converted from a large spot to a small one and a field converted from a small spot to a large one. The spotsize of the optical field emitted from the SSC was successfully expanded compared with that for an optical field emitted from the small-spot optical waveguide.

Table I summarizes the measured lateral and axial misalignment tolerances for a plane-ended PANDA SMF that has a spotsize of 4.1 $\mu$m. Misalignment tolerances for 1-dB down for the

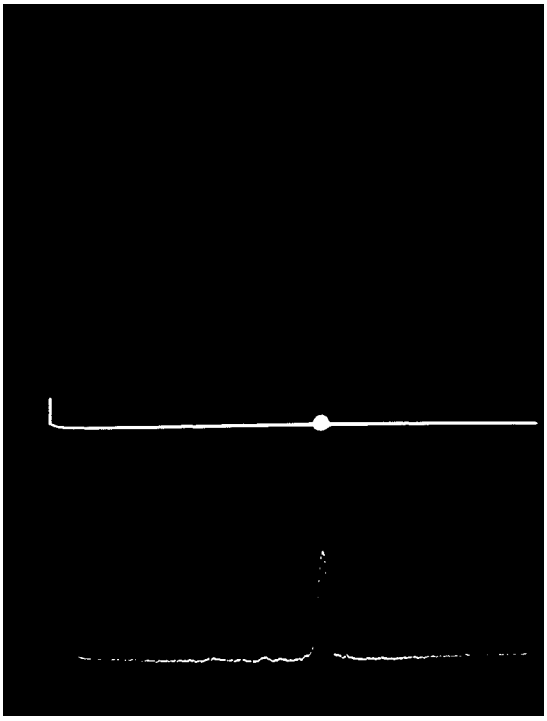

(a)

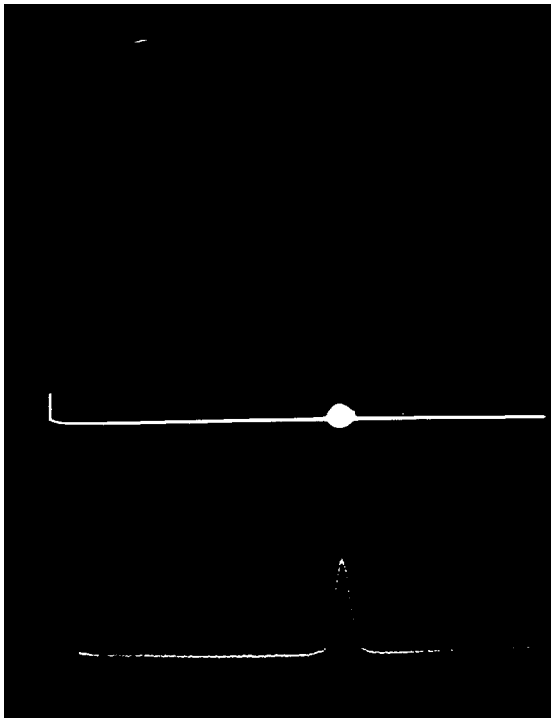

(b)

Fig. 11. Measured near-field patterns for: (a) a small-spot optical waveguide and (b) SSC.

SSC can successfully be expanded by three times in both the lateral and axial directions compared to those for the small-spot optical waveguide. This improvement of misalignment tolerances enables the fabrication of $2 \times 2$ and $4 \times 4$ switch modules with a UV-cure adhesive.

TABLE I

| Tolerances (μm/1-dB down) | | |
|---|---|---|
| axis \ SSC | without SSC | with SSC |
| x | ±0.8 | ±2.0 |
| y | ±0.7 | ±1.9 |
| z | 6 | 18 |

Fig. 12 shows the histogram for the sum of the measured spot-conversion loss and coupling loss. The results were obtained by subtracting the propagation loss from total insertion loss measured with two plane-ended SMF's for straight optical waveguides that have SSC's in the input and output ports. As shown in this figure, an average value of 2.3 dB was obtained for the sum of the coupling loss and spot-conversion loss for a facet.

### *B. Characteristics of* $2 \times 2$ *and* $4 \times 4$ *Switch Chips and Modules*

*1)* $2 \times 2$ *Switch:* The measured near-field pattern for a $2 \times 2$ optical waveguide switch chip is shown in Fig. 13. Crosstalk is small.

Fig. 14 shows the histogram of the measured total insertion loss for $2 \times 2$ switch chips including coupling loss between SSC's and plane-ended SMF's. Insertion loss of around 14 dB was obtained. Table I shows the loss budget of a fabricated typical $2 \times 2$ switch module, where "others" in the table means connector losses and loss increase at pig-tailing with UV cure adhesive. Fig. 15 shows the histogram for the loss variation at module assembly using UV-cure adhesive. Since the misalignment tolerances between the optical waveguides and SMF's were expanded by integrating the SSC's as shown in Table I, the loss variation at module assembling is small.

Fig. 16 shows measured insertion loss as a function of the applied voltage for the fabricated $2 \times 2$ switch module. The measured total insertion loss, including optical connector losses, was around 15 dB and crosstalk was less than $-20$ dB. The driving voltage was 7.0 V.

*2)* $4 \times 4$ *Switch:* Fig. 17 shows the measured near-field pattern for the $4 \times 4$ switch chip. Crosstalk was also small similarly to the $2 \times 2$ switch case.

Fig. 18(a) shows the measured insertion loss as a function of the applied voltage for the $4 \times 4$ switch module, where the optical field was coupled to the port of In 1 and SW4 in Fig. 1(b) was biased. Optical outputs from the four ports are shown. Measured connector-to-connector insertion losses were around 18–21 dB for all ports. Crosstalk was less than $-13$ dB and the switching voltage was from 9.2–9.8 V.

Fig. 18(b) shows the measured dynamic response of the $4 \times 4$ switch module for 10 Gbit/s optical pulses generated by a $LiNbO_3$ modulator using the same experimental setup as that in [20] and [22]. Optical power of $+3$ dBm was coupled to one of the input fibers. Then, a driving voltage of 9.8 V was applied. The optical outputs from two

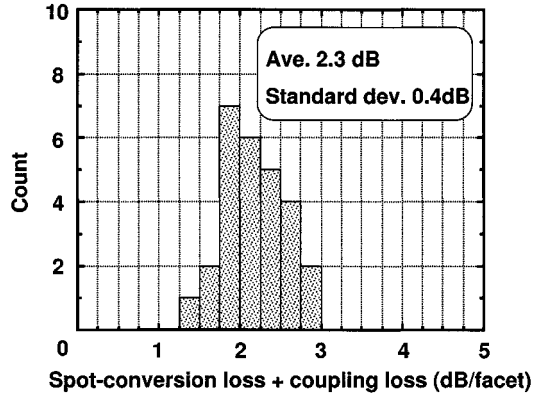


Fig. 12. Measured results of the sum of the spot- conversion loss and coupling loss.

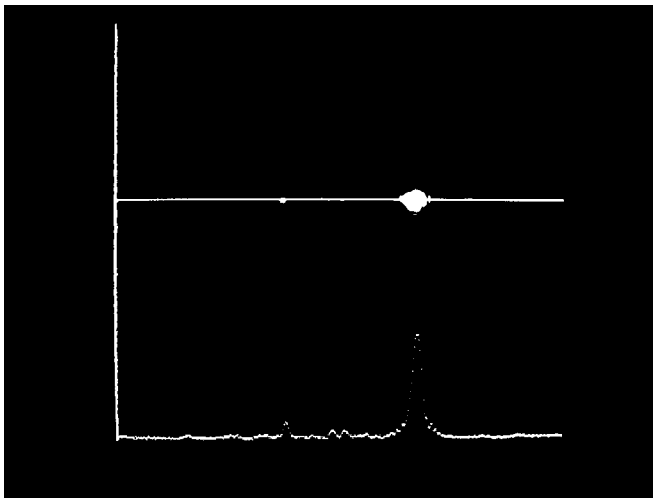

Fig. 13. Measured near-field pattern for a $2 \times 2$ optical waveguide switch chip.

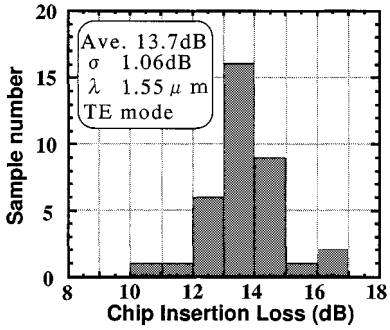


Fig. 14. Histogram of the measured total insertion loss for $2 \times 2$ switch chips including coupling loss between SSC's and plane-ended PANDA SMF's.

fibers were enhanced by a fiber amplifier and were coupled to an O/E receiver. Switching time was sufficiently short (<70 ps, which is limited by the driver speed) and no bits were lost during 10-Gb/s switching. Furthermore, crosstalk is sufficiently small. These high-speed switching characteristics were obtained for all switch elements. This device uses directional coupler-type switches, and therefore is polarization sensitive. By applying MZ and MMI couplers to the switches polarization insensitive characteristics can be obtained as demonstrated in [8] and [14]. The channel crosstalk of −13 dB is not low enough for packet switching, but this

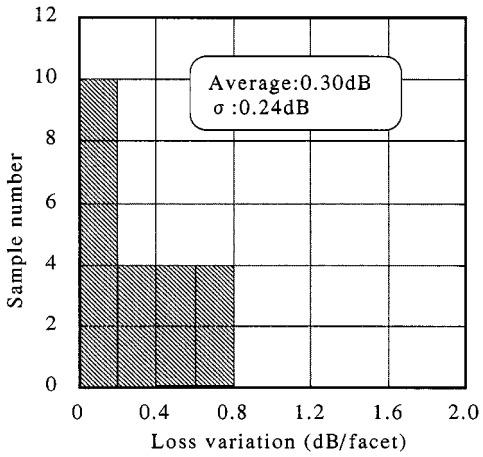


Fig. 15. Histogram of the loss variation at module assembling.

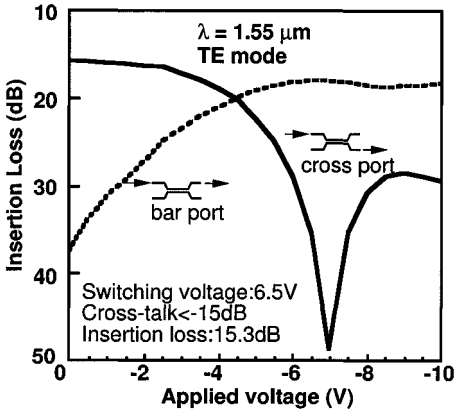


Fig. 16. Measured optical insertion loss as a function of the applied voltage for the $2 \times 2$ switch module.

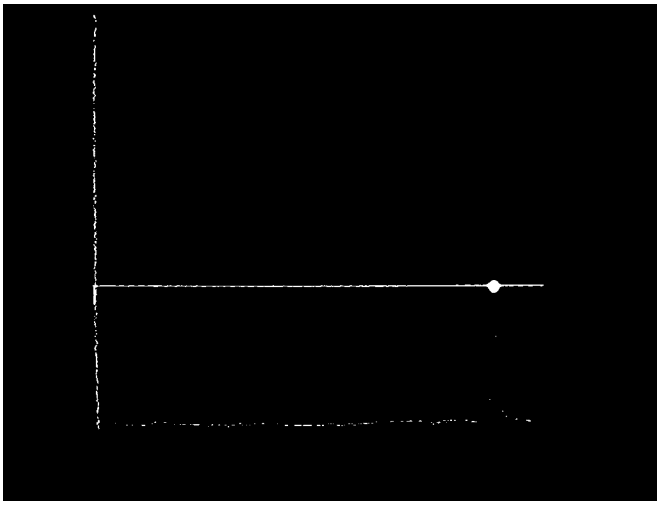

Fig. 17. Measured near-field pattern for the $4 \times 4$ switch chip.

is the first trial of the $4 \times 4$ SW and therefore we hope that we can improve the crosstalk characteristics, in the future.

## V. Conclusion

By integrating SSC's consisting of lateral tapers, thin-film cores, and ridges in InGaAlAs–InAlAs MQW directional

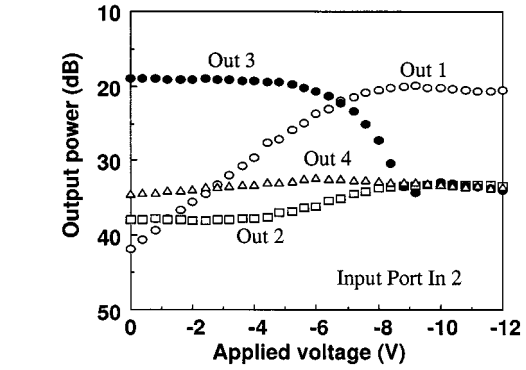


(a)

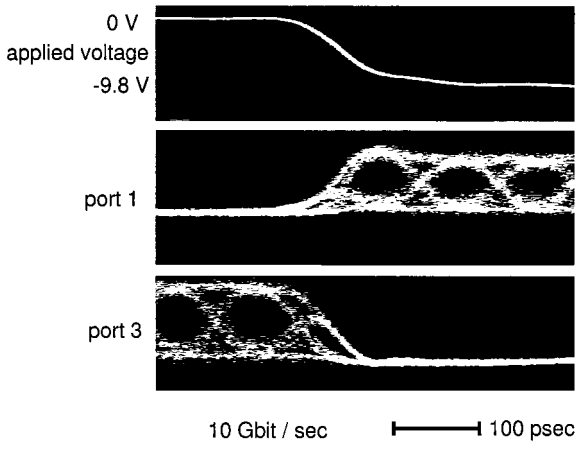


(b)

Fig. 18. (a) Measured optical insertion loss as a function of the applied voltage for the $4 \times 4$ switch module and (b) dynamic response for 10-Gb/s optical pulses for the $4 \times 4$ switch module.

coupler waveguide switches, fully-packaged $2 \times 2$ and $4 \times 4$ switch modules were successfully fabricated with a UV-cure adhesive. Good reproducibility was obtained for perfect coupling length of the directional coupler by appropriately designing the ridge width and gap of strip-loaded optical waveguides and by making use of the $Cl_2$ reactive-ion-beam-etching and successive wet-etching. In the SSC's, the 1.1 Q thin-film core confines the propagating beam in the vertical direction and the ridge confines it in the lateral direction. Since the switching time was sufficiently short (<70 ps, which was limited by the driver speed) for the $4 \times 4$ switch modules, no bits were lost during a 10-Gb/s switching experiment at a wavelength of 1.55 $\mu$m.

## ACKNOWLEDGMENT

The authors would like to thank H. Tsuchiya and J. Yoshida for their fruitful information and encouragement, and for providing the opportunity to conduct this research. They would also like to express their appreciation to N. Watanabe for his stimulating discussions and management as a group leader.

## REFERENCES

[1] C. G. M. Vreeburg, T. Uitterdijk, Y. S. Oei, M. K. Smit, F. H. Groen, J. J. G. M. van der Tol, P. Demeester, and H. J. Frankena, "Compact integrated InP-based add-drop multiplexer," in *Proc. 22nd Eur. Conf. Optic. Commun. (ECOC' 96)*, vol. 5, Oslo, Norway, 1996, pp. 67–70.

[2] A. Himeno, M. Okuno, Y. Ohmori, and M. Kawachi, "High extinction ratio $8 \times 8$ thermo-optic matrix switches using silica-based planar lightwave circuit," in *Proc. Topic. Meeting Photon. Switching*, 1996, Paper PThB3, p. 176.

[3] P. Granestrand, B. Lagerstrom, P. Svensson, H. Olofsson, J.-E. Falk, and B. Stolz, "Pigtailed tree-structured $8 \times 8$ LiNbO3 switch matrix with 112 digital optical switches," *IEEE Photon. Technol. Lett.*, vol. 6, pp. 71–73, 1994.

[4] K. Komatsu, K. Hamamoto, M. Sugimoto, A. Ajisawa, and A. Suzuki, "$4 \times 4$ GaAs/AlGaAs optical matrix switches with uniform device characteristics using alternating electroptic guided-wave directional couplers," *J. Lightwave Technol.*, vol. 9, pp. 871–878, 1991.

[5] H. Takeuchi, Y. Hasumi, S. Kondo, and Y. Noguchi, "$4 \times 4$ directional coupler switch matrix with an InGaAlAs/InAlAs multi quantum well structure," *Electron. Lett.*, vol. 29, pp. 52–524, 1993.

[6] J. E. Zucker, K. L. Jones, M. G. Young, B. I. Miller, and U. Koren, "Compact directional coupler switches using quantum well electro-refraction," *Appl. Phys. Lett.*, vol. 55, pp. 2280–2282, 1989.

[7] T. Aizawa, Y. Nagasawa, K. G. Ravikumar, and T. Watanabe, "Polarization-independent switching operation in directional coupler using tensile-strained multi-quantum well," *IEEE Photon. Technol. Lett.*, vol. 7, pp. 47–49, 1995.

[8] N. Yoshimoto, Y. Shibata, S. Oku, S. Kondo, Y. Noguchi, K. Wakita, K. Kawano, and M. Naganuma, "Fully polarization insensitive Mach–Zehnder optical switches using a wide-well InGaAlAs/InAlAs MQW structure," in *Proc. Photon. Switching*, Sendai, Japan, 1996, PWB 3.

[9] T. Kirihara, M. Ogawa, S. Tuji, and H. Inoue, "High-speed signal-transmission performance in a lossless $4 \times 4$ optical switch for photonic switching," in *Proc. Optic. Fiber Commun. (OFC)*, San Jose, CA, 1994, TuM3.

[10] M. Ikeda, S. Oku, Y. Shibata, T. Suzuki, and M. Okayasu, "Loss less $4 \times 4$ monolithic LD optical matrix switches," in *Proc. Int. Topic. Meeting Photon. Switching*, vol. 2D1, 1992, p. 792.

[11] L. Stoll, G. Muller, M. Honsberg, M. Schienle, J. Eichinger, and U. Wolff, "$4 \times 4$ optical matrix switch on InP with low switching current," *Archiv Fur Electronik Und Ubertragungstechnik*, vol. 46, pp. 116–118, 1992.

[12] J.-F. Vinchant, A. Goutelle, B. Martin, F. Gaborit, P. Pagnod-Rosiaux, J.-L. Peyre, J. LE. Bris, and M. Renaud, "New compact polarization insensitive $4 \times 4$ switch matrix on InP with digital optical switches, and integrated mirrors," in *Proc. Eur. Conf. Optic. Commun. (ECOC)*, Montreux, Switzerland, 1993, Postdeadline ThC12.4.

[13] W. H. Nelson, A. N. M. Masum Choudhury, M. Abdalla, R. Bryant, E. Meland, and W. Niland, "Wavelength-independent InP/InGaAsP digital optical switches with extinction ratio exceeding 20 dB at both 1.3 $\mu$m and 1.5 $\mu$m," in *Proc. Eur. Conf. Optic. Commun. (ECOC)*, Firenze, Italy, 1994, pp. 523–526.

[14] M. Bachmann, C. Nadler, P. A. Besse, and H. Melchior, "Compact polarization-insensitive multi-leg $1 \times 4$ Mach–Zehnder switch in InGaAsP/InP," in *Proc. Eur. Conf. Optic. Commun. (ECOC)*, Firenze, Italy, 1994, pp. 519–522.

[15] G. Muller, L. Stoll, G. Wegener, and M. Schienle, "First low loss InP/InGaAsP optical switch with integrated mode transformers," in *Proc. Eur. Conf. Optic. Commun. (ECOC)*, Montreux, , 1993, Postdeadline ThC12.10.

[16] R. Krahenbuhl, W. Bachmann, W. Vogt, T. Brenner, H. Duran, R. Bauknecht, W. Hunziker, R. Kyburz, C. Holtmann, E. Gini, and H. Melchior, "High-speed low-loss InP space switch matrix for optical communication systems, fully packaged with electronic drivers and single-mode fibers," in *Proc. Eur. Conf. Optic. Commun. (ECOC)*, Firenze, Italy, 1994, pp. 511–514.

[17] T. Ido, S. Tanaka, M. Suzuki, M. Koizumi, H. Sano, and H. Inoue, "Ultra-high-speed multiple-quantumn-well electro absorption optical modulators with integrated waveguides," *J. Lightwave Technol.*, vol. 14, pp. 2026–2034, 1996.

[18] N. Yoshimoto, K. Kawano, M. Kohtoku, S. Sekine, M. Yanagibashi, and S. Kondo, "The first demonstration of a $2 \times 2$ semiconductor switch module integrated with a spot size converter," in *Proc Integr. Photon. Res.*, 1994, SaC5-1.

[19] K. Kawano, M. Kohtoku, N. Yoshimoto, S. Sekine, and Y. Noguchi, "$2 \times 2$ InGaAlAs/InAlAs multiple-quantum well (MQW) directional coupler waveguide switch modules with spotsize converters," *Electron. Lett.*, vol. 30, pp. 353–354, 1994.
[20] T. Ito, M. Kohtoku, N. Yoshimoto, K. Kawano, S. Sekine, and M. Yanagibashi, "Dynamic response of $2 \times 2$ InGaAlAs/InAlAs multi-quantum well (MQW) directional coupler waveguide switch modules," *Electron. Lett.*, vol. 30, pp. 1936–1937, 1995.
[21] K. Kawano, S. Sekine, H. Takeuchi, M. Wada, M. Kohtoku, N. Yoshimoto, T. Ito, M. Yanagibashi, S. Kondo, and Y. Noguchi, "$4 \times 4$ InGaAlAs/InAlAs MQW directional coupler waveguide switch modules integrated with spotsize converters and their 10 Gbit/s operation," *Electron. Lett.*, vol. 31, pp. 96–97, 1995.
[22] T. Ito, M. Kohtoku, N. Yoshimoto, K. Kawano, S. Sekine, and M. Yanagibashi, "Dynamic response of InGaAlAs/InAlAs multiple quantum well (MQW) directional coupler waveguide switch module," in *Proc. Integr. Opt. Optic. Fiber Commun. (IOOC)*, 1995, Paper ThD1-1.
[23] R. Zengerle, O. Leminger, W. Weiershausen, K. Faltin, and B. Hubner, "Laterally tapered InP-InGaAsP waveguides for low-loss chip-to-fiber butt coupling: A comparison of different configuration," *IEEE Photon. Technol. Lett.*, vol. 7, pp. 532–534, 1995.
[24] T. Brenner, M. Bachmann, and H. Melchior, "Waveguide tapers for efficient coupling of InGaAsP/InP OEIC components to flat-end single mode fibers," in *Proc. Eur. Conf. Optic. Commun. (ECOC)*, Florence, Italy, 1994, pp. 1031–1034.
[25] M. Koshiba, H. Saitoh, M. Eguchi, and K. Hirayama, "Simple scalar finite element approach to optical rib waveguides," in *Proc. IEEE*, vol. 139, 1992, pp. 166–171.

**Masaki Kohtoku** was born in Kochi Prefecture, Japan, on March 16, 1966. He received the B.E. and M.E. degrees from the Department of Physical Electronics from the Tokyo Institute of Technology, Tokyo, Japan, in 1989 and 1991, respectively.

In 1991, he joined the NTT Opto-Electronics Laboratories, Kanagawa, Japan, where he is involved in research on semiconductor waveguide devices.

Mr. Kohtoku is a member of the Institute of Electronics, Information, and Communication Engineers (IEICE) of Japan and the Japan society of Applied Physics.

**Kenji Kawano** received the B.S. and M.S. degrees in physics and applied physics from Kyushu University, Fukuoka, Japan, in 1977 and 1979, respectively. He received the Ph.D. degree in 1989.

He joined Musashino Electrical Communication Laboratories, Nippon Telegraph and Telephone (NTT) Corporation, Tokyo, Japan, in 1979, and was engaged in research on thin-film waveguides for MIC's. Since 1982, his major efforts have been directed toward the research and development of optical devices for single-mode fiber transmission systems, with emphasis on semiconductor laser to single-mode fiber coupling modules. His work has also focused on the design and fabrication of $LiNbO_3$ high-speed waveguide modulators, multiple quantum-well (MQW) waveguide modulators, spotsize converter integrated laser diodes, and MQW waveguide switches. He is an author of two books entitled *Introduction and Application of Optical Coupling Systems to Optical Devices* (Japan: Gendai Kohgakusha, 2nd ed., 1998, in Japanese) and *Introduction to Optical Waveguide Analysis* (Japan: Gendai Kohgakusha, 1998, in Japanese, 1998). He is a Senior Research Engineer, Supervisor, at the NTT Opto-electronics Laboratories, Kanagawa, Japan.

Dr. Kawano is a member of the Institute of Electronics, Information and Communication Engineers (IEICE) of Japan and the Japan Society of Applied Physics.

**Satoshi Sekine** received the B.S. and M.S. degrees from Keio University, Tokyo, Japan, in 1978 and 1980, respectively.

In 1980, he joined NTT Electrical Communication Laboratories, Musashino, Tokyo, Japan, he has been engaged in the research and development on packaging technology of optical components.

Mr. Sekine is a member of the Japan Society of Applied Physics and the Institute of Electronics, Information and Communication Engineers (IEICE) of Japan.

**Hiroaki Takeuchi** was born in Mie, Japan, in 1957. He received the B.S., M.S., and Ph.D. degrees from Waseda University, Tokyo, Japan, in 1981, 1983, and 1991, respectively.

In 1983, he joined the Electrical Communication Laboratories, Nippon Telegraph and Telephone Public Corporation. Since then, he has been engaged in epitaxial growth of III–V semiconductor material and developing semiconductor optical integrated devices.

**Naoto Yoshimoto** (M'94) was born in Hokkaido, Japan, in 1963. He received the B.S. and M.S. degrees in electronics engineering from Hokkaido University, Japan, in 1986 and 1988, respectively.

In 1988, he joined the Opto-electronics Laboratories, Nippon Telephone and Telegraph Corporation, Kanagawa, Japan, where he was engaged in crystal growth and device fabrication of GaN-based blue laser diode, and he has been involved in research on the semiconductor-based waveguide optical devices such as switches, modulators, gates, and their integrated devices.

Mr. Yoshimoto is a member of the Japan society of Applied Physics, the Institute of Electronics, Information and Communication Engineers (IEICE) of Japan, and IEEE Lasers and Electro-Optics Society.

**Masato Wada** (M'92) received the B.S. and M.S. degrees in physics and the Ph.D. degree in electrical engineering from Waseda University, Tokyo, Japan, in 1974, 1977, and 1987, respectively.

In 1977, he joined NTT Electrical Communication Laboratory, Kanagawa, Japan, where he worked on Si-MOSFET circuit design and fabrication of the Josephson devices and compound semiconductor FET's. He has been engaged in research on fabrication of laser diodes and other photonic devices recently. He is now Senior Manager for the Research Planning Department, NTT Science and Core Technology Laboratory Group.

Dr. Wada is a member of the Institute of Electronics, Information and Communication Engineers (IEICE) of Japan, the Japan Society of Applied Physics, the IEEE Lasers and Electro-Optics Society (LEOS), and the Electrochemical Society.

**Toshio Ito** was born in Tokyo, Japan, in 1962. He received the B.S. and M.E. degrees from Keio University, Kanagawa, Japan, in 1984 and 1986, respectively.

In 1986, he joined the NTT Electrical Communication Laboratories, Tokyo, Japan, where he was engaged in research on parallel processing systems and communication switching systems. Since 1993, he has been engaged in research on the InGaAlAs–InAlAs MQW optical switches as well as the InGaAsP semiconductor optical amplifier gates at NTT Opto-electronics Laboratories, Kanagawa, Japan.

**Mitsuaki Yanagibashi**, photograph and biography not available the time of publication.

**Susumu Kondo** received the B.E. degree in electronics engineering from the Niigata University, Niigata, Japan, in 1972 and Dr.Eng. degrees from Kyoto University, Kyoto, Japan, in 1994.

In 1972, he joined NTT Electrical Communication Laboratories. He has been engaged in research and development on LPE, chloride VPE and MOVPE growth of $LiNbO_3$ and III–V semiconductor compounds, for optical devices. His current research includes MOVPE growth of MQW on InP for optical modulators and lasers. He is a Senior Research Engineer of Photonics Laboratory, NTT, Atsugi, Japan.

Dr. Kondo is a member of the Institute of Electrical Engineers of Japan and Applied Physics Society of Japan.

**Yoshio Noguchi** was born in Ibaragi, Japan, on July 2, 1948. He received the B.E. degree in electronic engineering from Tokyo Denki University, Tokyo, Japan, in 1974.

In 1967, he joined the Musashino Electrical Communication Laboratory, NTT Corporation, Tokyo, Japan, where he is engaged in research and development on LPE crystal growth techniques for optical semiconductor materials. Since 1983, he has been working at NTT Opto-electronics Laboratories, Kanagawa, Japan, and developing quaternary material crystals for light sources in lightwave communication system. He was also involved in the growth of the MOVPE techniques from 1991.

Mr. Noguchi is a member of the Japan Society of Applied Physics.

**Mitsuru Naganuma** (M'92) received the B.S. degree in electrical engineering from Yokohama National University, Yokohama, Japan, in 1971 and the M.S. and Ph.D. degrees from Tokyo Institute of Technology, Tokyo, Japan, in 1973 and 1976, respectively.

He joined NTT Electrical Communications Laboratories in 1976, and has been engaged in MBE growth and characterization of GaSb–AlSb and GaAs–AlGaAs superlattices and migration enhanced epitaxy of GaAs on Si. He was a Research Associate of the University of Southern California during 1984–1985. Since 1987, he has been engaged in research on photonic functional devices in NTT Opto-electronics Laboratories. Recent activities include research on semiconductor photonic devices.

Dr. Naganuma is a member of Institute of Electronics, Information and Communication Engineers (IEICE) of Japan, the Japan Society of Applied Physics, and the Institute of Electrical Engineers of Japan.